

Chapter 24

Influence of Jute Fibers to Improve Flexural Toughness, Impact Resistance and Drying Shrinkage Cracking in Adobe Mixes



Jose Concha-Riedel, Gerardo Araya-Letelier, Federico C. Antico, Ursula Reidel and Andres Glade

24.1 Introduction

Revival of interest in the use of earthen construction materials can be seen over the last few decades due to the advantages such as thermal comfort, greenness and low environmental impacts (Cataldo-Born et al. 2016; Donkor and Obonyo 2015; Millogo et al. 2014; Minke 2006). However, earthen materials also have disadvantages such as low mechanical strength, poor erosion resistance and drying shrinkage cracking (Avrami et al. 2008; Minke 2000, 2006). The incorporation of industrialized fibers, such as polypropylene fibers (Donkor and Obonyo 2015; Yilmaz 2009), and of natural fibers, such as straw and even wool (Aymerich et al. 2012; Quagliarini and Lenci 2010), has been studied to mitigate some of the disadvantages of earthen materials. Among natural fibers, there have been recent studies addressing the use of jute fibers. Islam et al. (2008) studied the impact of natural fibers, including jute fibers, on strength and toughness of earthen blocks as well as shrinkage cracking of mortars

J. Concha-Riedel
Universidad Adolfo Ibañez, Santiago, Chile
e-mail: jose.concha@uai.cl

G. Araya-Letelier (✉)
Pontificia Universidad Católica de Chile, Santiago, Chile
e-mail: gerardo.araya@uc.cl

F. C. Antico · A. Glade
Universidad Adolfo Ibañez, Viña del Mar, Chile
e-mail: federico.antico@uai.cl

A. Glade
e-mail: aglade@alumnos.uai.cl

U. Reidel
Sika S.A. Chile, Santiago, Chile
e-mail: reidel.ursula@cl.sika.com

© Springer Nature Singapore Pte Ltd. 2019
B. V. V. Reddy et al. (eds.), *Earthen Dwellings and Structures*,
Springer Transactions in Civil and Environmental Engineering,
https://doi.org/10.1007/978-981-13-5883-8_24

Table 24.1 Morphological, physical and mechanical properties of jute fiber after Daniel et al. (2002)

Diameter (mm)	Specific gravity	Modulus of elasticity (MPa)	Tensile strength (MPa)	Elongation at break (%)
0.102–0.203	1.02–1.04	25,990–31,992	250–350	1.5–1.9

and jute was found to be the most effective fiber, improving strength and toughness as well as preventing shrinkage cracking. Güllü and Khudir (2014) studied the effect of natural fibers, including jute fibers, on the unconfined compressive strength of fine-grained soil subjected to freeze-thaw cycles, and it was found that the incorporation of jute fiber increased both non-freeze-thaw and freeze-thaw unconfined compressive strengths compared to unreinforced soil. Saleem et al. (2016) assessed the effect of jute fiber on the compressive strength of earth bricks finding increments of compressive strength due to the incorporation of jute fiber. Although the contribution of the studies addressing the reinforcement of earthen materials with jute has been significant, there are still some properties that have not been studied intensely and quantitatively, such as impact resistance.

The novelty of this research resides in the incorporation of jute fiber into earthen materials such as adobe mixes, addressing quantitatively the impact of the incorporation of jute into flexural toughness, impact resistance and drying shrinkage cracking. This study has the following objectives: to evaluate the influence of different lengths and dosages of jute fiber on (i) flexural strength, (ii) flexural toughness, (iii) drying shrinkage performance and (iv) impact resistance in adobe mixes.

24.2 Materials and Methods

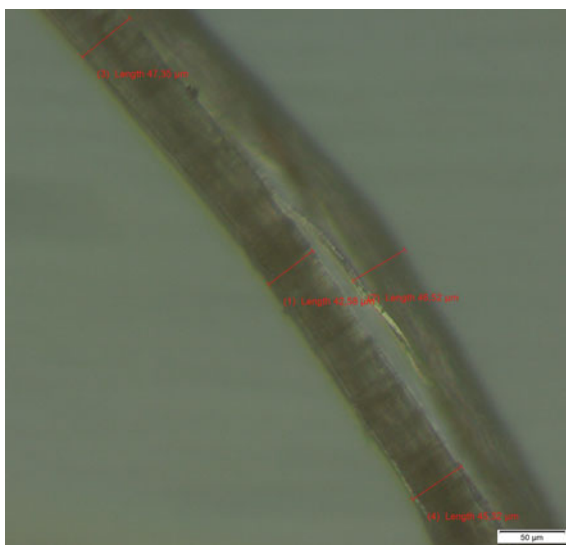
24.2.1 Materials

The present study uses a clayey soil from a district in Santiago, Chile. Araya-Letelier et al. (2018) conducted a characterization of the same soil, obtaining an 11%, 69% and 20% of clay, silt and sand, respectively. The liquid and plastic Atterberg limits, plasticity index and specific gravity of solids were also characterized, and their values are 29.1%, 17.4%, 11.7% and 2.51% respectively.

Jute is used as a natural reinforcing fiber for adobe mixes, and Table 24.1 summarizes some of the most relevant morphological, physical and mechanical properties of this vegetal fiber reported by Daniel et al. (2002).

The jute fiber used in this study was processed to obtain three different lengths (7, 15 and 30 mm) to perform a sensitivity analysis on the impact of different lengths and dosages of fibers on the performance of adobe mixes. Considering the range of diameters (0.1–0.2 mm) reported by Daniel et al. (2002) and the three different

Fig. 24.1 Microscopy of jute fibers



lengths used in this study, the ranges of aspect ratios to be used are 35–70, 75–150 and 150–300 for fiber lengths of 7, 15 and 30 mm, respectively. Figure 24.1 shows a microscopy of the jute fibers.

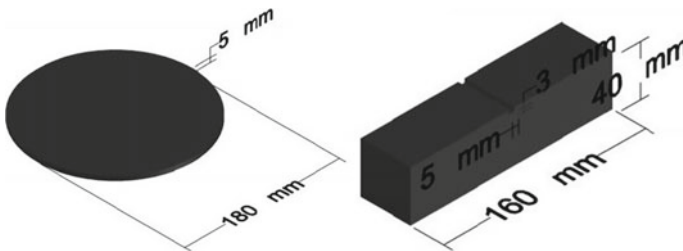
24.2.2 Adobe Mix Proportions and Specimen Preparation

A water-to-soil ratio (i.e., the weight of water to the weight of dry soil) of 0.307 was determined based on the required workability of the mixes. Seven different adobe mixes were cast for this investigation, six of them incorporating fiber and one plain mix, to make comparisons between them. The six jute-reinforced mixes had two dosages (0.5 and 2% by mass of soil) and three different fiber lengths (7, 15 and 30 mm). The different adobe mix ID numbers and fiber dosages are presented in Table 24.2, where the identification number (ID) indicates first the dosage and second the length of the fiber.

The adobe mixes and the specimens were carried out manually. The fibers were mixed initially with the dry soil, until all clusters were disassembled. After all the fibers were included into the soil, water was added into the mixture in four equal portions, mixing after each incorporation. Finally, the adobe mixes were covered with a plastic bag to prevent water evaporation. The following specimens were cast for each adobe mix: (i) six notched RILEM beam specimens (160 mm × 40 mm × 40 mm, according to ISO/R679 (1968)) for impact strength test, (ii) six RILEM beam specimens for flexural strength, toughness indices and residual strength factors and (iii) two cylindrical specimens for drying shrinkage cracking. After 48 h, the

Table 24.2 Adobe mix ID number and material proportion

Adobe mix ID	Fiber (%)	Fiber length (mm)
0–0	0	0
0.5–7	0.5	7
0.5–15	0.5	15
0.5–30	0.5	30
2.0–7	2.0	7
2.0–15	2.0	15
2.0–30	2.0	30

**Fig. 24.2** Cylindrical specimen (right) and RILEM beam specimen (left) after Araya-Letelier et al. (2018)

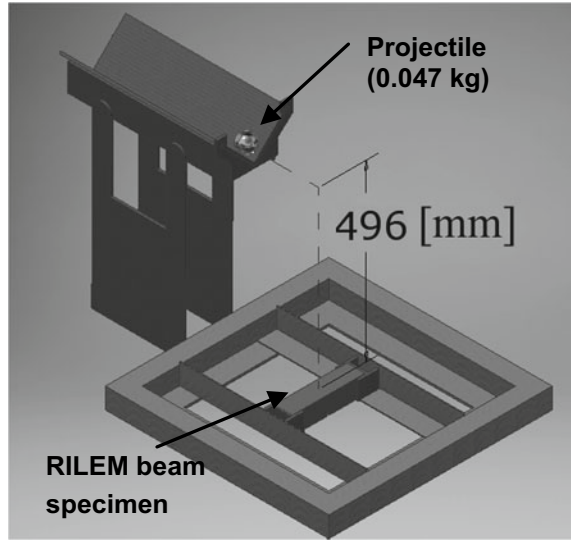
specimens were demolded and kept at laboratory conditions (22 °C and 45% relative humidity) for 28 days until testing, rotating to the adjacent side 90° every 7 days. A fine coat of glue and sand was applied in the molds of the cylindrical specimens for ease of de-molding. The specimens for shrinkage crack testing were kept at laboratory conditions (22 °C and 45% relative humidity) for seven days in the molds, and cracking was measured afterward. Sketches in Fig. 24.2 show dimensions of the specimens.

24.2.3 Testing

Flexural strength of each adobe mix was assessed at 28 days after casting using a three-point bending configuration over six RILEM beam specimens with a span of 130 mm between supports and using a displacement control protocol with a rate of 1 mm/minute.

To assess the energy absorption capacity of each adobe mix, flexural toughness indices were calculated according to ASTM C1018 (1997) procedure. The flexural toughness indices were calculated as the area under the load-deflection curve up to a specific deflection value divided by the area under the load-deflection curve up to the deflection where the first crack was observed (δ). Specifically, flexural toughness indices I_5 , I_{10} and I_{20} are the values obtained using deflections of 3δ , 5.5δ and

Fig. 24.3 Impact test setup after Araya-Letelier et al. (2018)



10.5 δ , which are stated in ASTM C1018 (1997), respectively. Moreover, the residual strength factors, representing the average post-crack load retained over a deflection interval as a percentage of the load at the first crack, were estimated directly from the flexural toughness indices using Eqs. (24.1) and (24.2) (for further information, see ASTM C1018 (1997)).

$$R_{5,10} = 20(I_{10} - I_5) \quad (24.1)$$

$$R_{10,20} = 10(I_{20} - I_{10}) \quad (24.2)$$

where $R_{5,10}$ and $R_{10,20}$ are the residual strength factors between the intervals of 5.5 δ and 3 δ , and 10.5 δ and 5.5 δ , respectively. Mean and standard deviation of toughness indices and average residual strength factors for each adobe mix were obtained from the individual flexural load-displacement curves at 28 days after casting.

To measure the drying shrinkage cracking, widths and lengths were measured using a crack width comparator and a caliper, guided by a 20 \times 20 mm grid, which was drawn on the surface of specimens. Crack width reduction ratio (CWRR) was calculated with respect to plain adobe, as well as crack width average (CWA) for all dosages.

To assess the impact energy absorption of the adobe mix after an age of 28 days, a projectile was thrown to the center of a RILEM beam specimen with a notch in the middle section as presented in Fig. 24.3. To avoid damage due to rebound, the specimens were glued with silicone to the steel frame. The impact energy was calculated using Eq. (24.3).

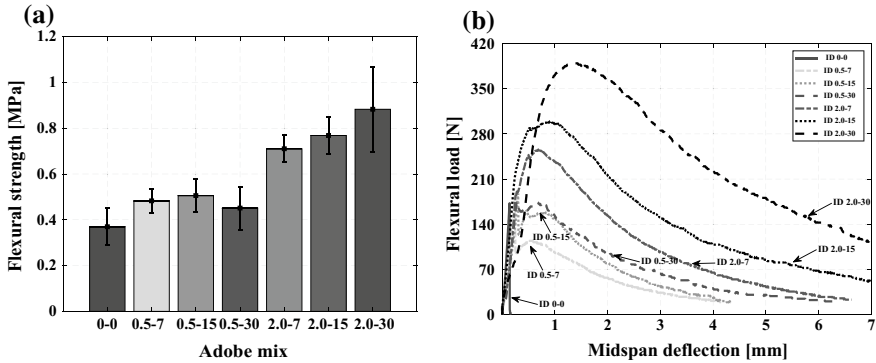


Fig. 24.4 a Flexural strength results and b compressive strength results

$$E_C = n * m * g * h \tag{24.3}$$

where E_C stands for the total energy at failure of the specimen, n is the required number of blows to cause failure to the specimen, m is the mass of the projectile (0.047 kg), g is the gravitational constant (9.8 m/s²), and h is the height of the fall of the projectile (0.496 m).

24.3 Results and Discussion

24.3.1 Flexural Strength, Toughness Indices and Residual Strength Factors

The results for flexural strength are presented in Fig. 24.4a, along with the error bars, considering one standard deviation above and below the mean value. Plain adobe had the worst flexural strength (0.37 MPa), whereas adobe mix ID 2.0–30 had the strongest flexural strength (0.88 MPa). Adobe mix ID 0.5–7 presented the less scattered data (SD = 0.05 MPa), whereas the most scattered data was obtained for adobe mix ID 2.0–30 (SD = 0.19 MPa). Analyzing the error bars, if the SD value of mix ID 0–0 is added to the mean, and the SD value of mix ID 2.0–30 is subtracted from the mean, the resulting value is still larger for ID 2.0–30. The latter might indicate that the length and dosage of jute fiber in adobe mixes do increase its flexural strength. The increase in flexural strength when jute is incorporated might be explained by the adequate mixing of the fibers and the satisfactory bonding between long fibers and the matrix.

Typical load-deflection curves are presented in Fig. 24.4b for each adobe mix, tested as mentioned in Sect. 2.3. Figure 24.4b shows that initially, the flexural stress increases linearly at the same stress-deflection rate until a visible crack is observed

Table 24.3 Toughness indices and residual strength factors at 28 days after casting

Adobe mix ID	I_5		I_{10}		I_{10}		$R_{5,10}$	$R_{10,20}$
	Avg ¹	SD ²	Avg ¹	SD ²	Avg ¹	SD ²	Avg ¹	Avg ¹
0-0	1.16	0.14	1.16	0.14	1.16	0.14	0.0	0.0
0.5-7	6.28	5.47	9.85	5.78	13.64	4.30	71.38	37.90
0.5-15	4.38	0.80	7.98	1.93	12.45	3.81	71.99	44.68
0.5-30	3.76	0.97	5.84	2.74	8.24	5.82	41.45	24.03
2.0-7	3.50	0.24	5.10	0.59	6.23	1.08	32.19	11.26
2.0-15	3.54	0.73	5.32	1.62	6.71	2.61	35.53	13.88
2.0-30	3.10	0.32	4.29	0.63	4.82	1.10	23.67	5.32

¹Average; ²standard deviation

growing from the lower surface of the sample (under tension). The later occurs regardless of the fiber dosage, which indicates that up to the peak load, the flexural response of the adobe mixes depends on the mechanical behavior of the matrix mainly, which is considered as brittle. After reaching the peak load, adobe mix ID 0 presents a brittle failure mode, whereas fiber-reinforced adobe mixes present an enhanced post-peak performance.

Table 24.3 presents average and SD values of I_5 , I_{10} and I_{20} and the average values of residual strength factor for each adobe mix. It can be seen that all the values of toughness indices (I_5 , I_{10} , and I_{20}) for adobe mix ID 0-0 are approximately 1.0, which means that this adobe mix has a brittle mode of failure where its flexural strength is followed by a sudden drop of the mechanical load joined by unstable macroscopic crack formation. In contrast, all the fiber-reinforced adobe mixes exhibit a load recovery after the first crack, joined by an increment of the mid-span deflection before failure, and toughness indices as well as residual strength factors increase mainly due to the presence of jute fibers.

24.3.2 Restrained Drying Shrinkage Distributed Cracking

The results of the drying shrinkage cracking can be seen in Fig. 24.5, where one of the two shrinkage specimens is shown. As can be seen, cracking is consistently reduced as the fiber length and dosage is increased. The CWA values of mix ID 0-0 and ID 2.0-30 were 1.2 and 0.2 mm, respectively.

CWA and CWRR results for each adobe mix are shown in Fig. 24.6 in the left side axis and right side axis, respectively. As was qualitatively observed in Fig. 24.5, the average width of the cracks, as well as the reduction ratio, is sensitive to the dosage and length of the fiber. ID 0-0 presented average values of crack width of 0.84 mm, whereas results for adobe mixes with jute fiber oscillated between 0.26 mm (ID 0.5-7) and 0.13 mm (ID 2.0-30). The corresponding CWRR values were 68 and

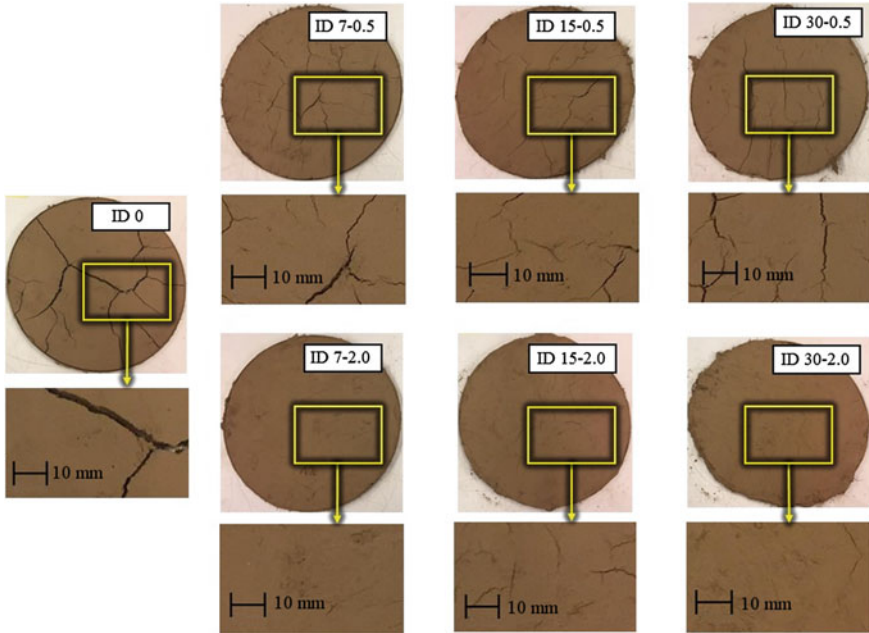
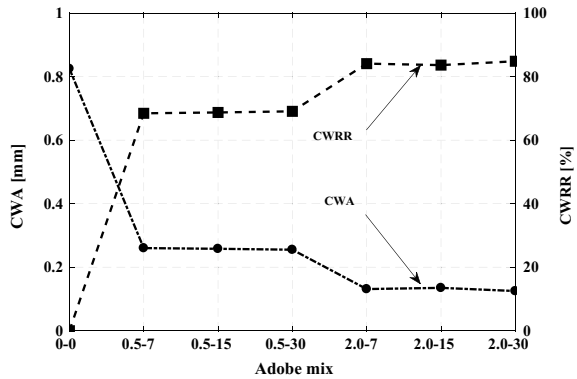
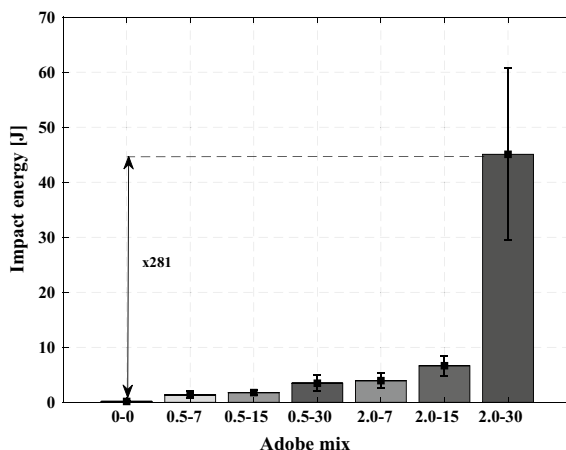


Fig. 24.5 Restrained drying shrinkage cracking results

Fig. 24.6 CWA and CWRR results



86%, respectively. As can be observed in Fig. 24.6, the CWRR results might indicate a higher sensitivity for fiber dosage than fiber length, where the increment for length is two percentage points and approximately 15 percentage points for increment of dosage. Antico et al. (2012) studied the behavior of material matrixes and the failure mechanisms for fibers, which is consistent with the effects observed by naked eye in this experiment. As the fiber dosages were increased, the characteristic length between the fiber and the matrix is reduced, increasing the chances that fibers are scattered throughout the matrix.

Fig. 24.7 Cumulative collapse impact energy

24.3.3 Impact Strength

Mean results of the impact test energy absorption are shown in Fig. 24.7, as well as error bars corresponding to one standard deviation above and below the mean. It can be observed that as the fiber length and dosage is increased, the energy absorption also increases. Adobe mix ID 0.5–15 and ID 2.0–30 show average results of 2.17 and 38 J (16 and 281 times the energy required to collapse plain adobe), respectively. As was studied by Araya-Letelier et al. (2017), quasi-brittle materials like mortars are expected to enhance its toughness when natural fibers are incorporated into the matrix. Like mortars, reinforced adobe could behave as a quasi-brittle material, and likewise, as fibers are incorporated it is expected that its energy-absorbing capacity is improved.

24.4 Conclusions

The results show that there is an improvement in the flexure strength of jute fiber-reinforced adobe mixes when compared with those of plain adobe specimens. The jute fiber reinforcement also resulted in an increase of flexural toughness. Incorporation of jute fibers reduced crack widths. The energy absorption due to impact was considerably enhanced by the incorporation of jute fibers. The impact energy absorption capacity of adobe mixes with jute fibers is sensitive to the length as well as fiber content.

Acknowledgements The authors would like to thank Arnaldo Puebla and Sabine Kunze, for the help provided for the sample preparation, and Sika S.A. Chile, for the use of their facilities for part of the experimental work presented.

References

- Antico FC, Zavattieri PD, Hector LG Jr, Mance A, Rodgers WR, Okonski DA (2012) Adhesion of nickel–titanium shape memory alloy wires to thermoplastic materials: theory and experiments. *Smart Mater Struct* 21(3):035022
- Araya-Letelier G, Antico FC, Carrasco M, Rojas P, García-Herrera CM (2017) Effectiveness of new natural fibers on damage-mechanical performance of mortar. *Constr Build Mater* 152:672–682
- Araya-Letelier G, Concha-Riedel J, Antico FC, Valdés C, Cáceres G (2018) Influence of natural fiber dosage and length on adobe mixes damage-mechanical behavior. *Constr Build Mater* 174:645–655
- ASTM C1018 (1997) Standard test method for flexural toughness and first-crack strength of fiber-reinforced concrete (using beam with third-point loading) (withdrawn 2006)
- Avrami EC, Guillaud H, Hardy M (eds) (2008) *Terra literature review: an overview of research in earthen architecture conservation*. Getty Conservation Institute, Los Angeles
- Aymerich F, Fenu L, Meloni P (2012) Effect of reinforcing wool fibres on fracture and energy absorption properties of an earthen material. *Constr Build Mater* 27(1):66–72
- Cataldo-Born M, Araya-Letelier G, Pabón C (2016) Obstacles and motivations for earthbag social housing in Chile: energy, environment, economic and codes implications. *Revista de La Construcción* 15(3):17–26
- Daniel JI, Ahmad SH, Arockiasamy M, Ball HP et al (2002) State-of-the-art report on fiber reinforced concrete. Reported by ACI Committee 544. Farmington Hills, MI
- Donkor P, Obonyo E (2015) Earthen construction materials: assessing the feasibility of improving strength and deformability of compressed earth blocks using polypropylene fibers. *Mater Des* 83:813–819
- Güllü H, Khudir A (2014) Effect of freeze–thaw cycles on unconfined compressive strength of fine-grained soil treated with jute fiber, steel fiber and lime. *Cold Reg Sci Technol* 106:55–65
- Islam MS, Iwashita K, Rahman MM (2008) Performance of natural fiber reinforced soil in earthen houses. In: *Proceedings of the sixth Asian young geotechnical engineers conference*, Bangalore, India, Paper No. CP, vol 22
- ISO/R679 (1968) *Méthode d'essais mécaniques des ciments. Resistance á la compression et á la flexion du mortier plastique (Méthode RILEM-CEMBUREAU)*
- Millogo Y, Morel JC, Aubert JE, Ghavami K (2014) Experimental analysis of Pressed Adobe Blocks reinforced with *Hibiscus cannabinus* fibers. *Constr Build Mater* 52:71–78
- Minke G (2000) *Earth construction handbook: the building material earth in modern architecture*. WIT Press, Southampton
- Minke G (2006) *Building with Earth: design and technology of a sustainable architecture*. Walter de Gruyter
- Quagliarini E, Lenci S (2010) The influence of natural stabilizers and natural fibres on the mechanical properties of ancient Roman adobe bricks. *J Cult Heritage* 11(3):309–314
- Saleem MA, Abbas S, Haider M (2016) Jute fiber reinforced compressed earth bricks (FR-CEB)—a sustainable solution. *Pak J Eng Appl Sci* 19:83–90
- Yilmaz Y (2009) Experimental investigation of the strength properties of sand–clay mixtures reinforced with randomly distributed discrete polypropylene fibers. *Geosynthetics Int* 16(5):354–363